Titre: Title:	Lysosomal rupture induced by structurally distinct chitosans either promotes a type 1 IFN response or activates the inflammasome in macrophages
Auteurs: Authors:	David Fong, Pascal Grégoire-Gélinas, Alexandre P. Cheng, Tal Mezheritsky, Marc Lavertu, Sachiko Sato, & Caroline D. Hoemann
Date:	2017
Type:	Article de revue / Article
Référence: Citation:	Fong, D., Grégoire-Gélinas, P., Cheng, A. P., Mezheritsky, T., Lavertu, M., Sato, S., & Hoemann, C. D. (2017). Lysosomal rupture induced by structurally distinct chitosans either promotes a type 1 IFN response or activates the inflammasome in macrophages. Biomaterials, 129, 127-138. https://doi.org/10.1016/j.biomaterials.2017.03.022

Biomaterials 129 (2017) 127–138

Contents lists available at ScienceDirect

Biomaterials

journal homepage: www.elsevier.com/locate/biomaterials

Lysosomal rupture induced by structurally distinct chitosans either promotes a type 1 IFN response or activates the inflammasome in macrophages

David Fong, Ph.D. [a], Pascal Grégoire-Gélinas [b], Alexandre P. Cheng, B.Eng. [b], Tal Mezheritsky [b], Marc Lavertu, Ph.D. [b], Sachiko Sato, Ph.D. [c], Caroline D. Hoemann, Ph.D., P.Eng. [a, b, d, *]

[a] Institute of Biomedical Engineering, École Polytechnique, Montreal, QC, H3T 1J4, Canada
[b] Department of Chemical Engineering, École Polytechnique, Montreal, QC, H3T 1J4, Canada
[c] Research Centre for Infectious Diseases, Faculty of Medicine, Laval University, Quebec, QC, G1V 4G2, Canada
[d] FRQ-S Biomedical Research Group/ Groupe de Recherche en Sciences et Technologies Biomédicales, École Polytechnique, Montreal, QC, H3T 1J4, Canada

ARTICLE INFO

Article history:
Received 30 November 2016
Received in revised form
20 February 2017
Accepted 14 March 2017
Available online 15 March 2017

Keywords:
Chitin/chitosan
Macrophage
Immunomodulation
Inflammasome
Type 1 interferon

ABSTRACT

Chitosan is a family of glucosamine and *N*-acetyl glucosamine polysaccharides with poorly understood immune modulating properties. Here, functional U937 macrophage responses were analyzed in response to a novel library of twenty chitosans with controlled degree of deacetylation (DDA, 60–98%), molecular weight (1 to >100 kDa), and acetylation pattern (block vs. random). Specific chitosan preparations (10 or 190 kDa 80% block DDA and 3, 5, or 10 kDa 98% DDA) either induced macrophages to release CXCL10 and IL-1ra at 5–50 μg/mL, or activated the inflammasome to release IL-1β and PGE_2 at 50–150 μg/mL. Chitosan induction of these factors required lysosomal acidification. CXCL10 production was preceded by lysosomal rupture as shown by time-dependent co-localization of galectin-3 and chitosan and slowed autophagy flux, and specifically depended on IFN-β paracrine activity and STAT-2 activation that could be suppressed by PGE_2. Chitosan induced a type I IFN paracrine response or inflammasome response depending on the extent of lysosomal rupture and cytosolic foreign body invasion. This study identifies the structural motifs that lead to chitosan-driven cytokine responses in macrophages and indicates that lysosomal rupture is a key mechanism that determines the endogenous release of either IL-1ra or IL-1β.

1. Introduction

Chitosan represents a family of a linear polysaccharide of β-*O*-(1–4)-linked glucosamine (GlcN) with variable content of *N*-acetyl glucosamine (GlcNAc). Chitosan is used in medical devices for hemostasis and regenerative medicine through mechanisms involving macrophage immune responses that have yet to be thoroughly elucidated [1–3]. To fully exploit the potential of this biomaterial polymer in regenerative medicine, its immunological properties should be thoroughly understood. Despite multiple studies that investigated macrophage responses to chitosan [3–14], current models are unable to explain why a given chitosan may elicit pro- or anti-inflammatory responses in macrophages. For example, chitosan has been shown to be a potent activator of the inflammasome [4,5], and can promote the release of pro-inflammatory cytokines Interleukin-1β (IL-1β) [4–6], Tumor Necrosis Factor (TNF) and chemokines associated with M1 macrophage polarization [6,8]. Conversely, chitosan can also elicit anti-inflammatory M2 macrophages [3,11], and stimulate the release of anti-inflammatory cytokines Interleukin-1 receptor antagonist (IL-1ra) and IL-10 [6,10]. Others have also reported that certain types of chitosan are relatively immunologically inert [13,14]. Across these studies, chitosans of varying origins, structural properties and purities were used. What is lacking at this time is a structure-function model that can be used to predict macrophage responses to chitosan according to its 3 main molecular characteristics: molecular weight, degree of deacetylation (DDA), and acetylation pattern.

* Corresponding author. Department of Chemical Engineering, 2900 boul. Édouard-Montpetit, École Polytechnique, Montréal, QC, H3C 3A7, Canada.
E-mail address: caroline.hoemann@polymtl.ca (C.D. Hoemann).

http://dx.doi.org/10.1016/j.biomaterials.2017.03.022

Chitosan is produced by chemical deacetylation of chitin $(GlcNAc\beta1\text{-}4)_n$ [15], leading to chitosan preparations with a GlcN content or DDA that ranges from 50 to 100%. In chitosans produced by this approach, the remaining GlcNAc residues are arranged in block, or clusters that are distributed heterogeneously along the chitosan chain [16]. Chitosan may also be produced with a random, homogeneous distribution of GlcNAc residues by treating fully deacetylated chitosan $(GlcN\beta1\text{-}4)_n$, with acetic anhydride which reacetylates chitosan to specific DDA levels [17,18]. Chitosan can also be depolymerized with nitrous acid to target molecular weights with acceptable polydispersity (PDI, weight-average molecular weight (M_w)/number-average molecular weight (M_n)) [19]. These methods can be used to produce chitosans with controlled structural features.

In a previous study, we analyzed the effects of a 132 kDa, 82% DDA, block-acetylated chitosan on the release of multiple pro- and anti-inflammatory cytokines, chemokines and growth factors in M0, M1 and M2-polarized U937 human macrophages. In non-polarized macrophages, we found that chitosan selectively induced the release of a pro-inflammatory cytokine (IL-1β), a mesenchymal stem cell chemokine (CXCL10) and an anti-inflammatory cytokine (IL-1ra) [6]. CXCL10 release was mediated by STAT-1 signaling and triggered in a delayed fashion by this 82% DDA chitosan. By contrast, 128 kDa 98% DDA chitosan failed to induce CXCL10 release for reasons that remain unclear [6]. 82% DDA chitosan-enhanced IL-1ra release was shown to be independent of paracrine IL-4, IL-10 signaling and IL-1β release [6], suggesting that this effect is mediated by signaling pathways that remain to be determined. Furthermore, these findings also raise the possibility that chitosan structural properties can be tailored to elicit specific cytokine responses without eliciting others, such as inducing IL-1ra release without stimulating the release of IL-1β. The purpose of this study was to understand the mechanisms behind chitosan-induced cytokine production, in non-polarized macrophages.

Several studies have compared macrophage responses to 2 or 3 chitosans with different DDA [6,11], or different molecular weight [6,12,13]. A systematic and comprehensive study of pro- and anti-inflammatory macrophage responses to a library of chitosans with distinct DDA and a comprehensive range of molecular weights is currently lacking. In this work, we generated a library of twenty different chitosans, with DDAs of 60, 80 and 98%, discrete number-average molecular weights (M_n) of 1 to over 100 kDa, with block or random acetylation patterns. This library was used to identify the minimal structural properties required for chitosan to stimulate macrophages to produce IL-1ra, CXCL10, IL-1β and Prostaglandin E_2 (PGE_2). These 4 factors were intended to serve as markers of chitosan-induced anti-inflammatory (IL-1ra), chemokine (CXCL10) or pro-inflammatory (IL-1β, PGE_2) responses in non-polarized U937 cells [6]. We then investigated the cellular mechanisms that lead to distinct cytokine responses and identified lysosomal disruption and IFN-beta (IFN-β) as the paracrine signaling pathway responsible for enhanced release of IL-1ra and CXCL10.

2. Material and methods

2.1. Reagents

RPMI-1640, fetal bovine serum (FBS), LysoTracker® Green DND-26, Alexa Fluor 488 donkey anti-mouse IgGs and Hoechst 33342 were purchased from Thermo Fisher Scientific (Burlington, ON, Canada). Recombinant human IL-4, IFN-α, IFN-β, IFN-γ, neutralizing antibodies against IFN-α (Clone MMHA-11) and IFN-β (#AF814), and enzyme-linked immunosorbent assay (ELISA) kits for IL-1β, IL-1ra and CXCL10/IP-10 were purchased from R&D Systems (Minneapolis, MN, USA). Express ELISA kits for PGE_2 were purchased from Cayman chemical (Ann Arbor, MI, USA). Antibodies for phosphorylated STAT-1 (#7649, Tyr701, clone D4A7), STAT-1 (#9172), LC3A/B (#12741, Clone D3U4C), Alexa Fluor 647-conjugated LC3A/B (#13394), β-Actin and horseradish peroxidise (HRP)-conjugated goat anti-rabbit secondary antibodies were purchased from New England Biolabs (Cell Signaling Technologies, Pickering, ON, Canada). Antibodies for phosphorylated STAT-2 (#07-224, Tyr689) and STAT-2 (#07-140) were purchased from EMD Millipore (Etobicoke, ON, Canada). Mouse monoclonal antibody for Galectin-3 (Clone B2C10) was purchased from BD Biosciences (Mississauga, ON, Canada). EDTA-free Complete™ protease inhibitor cocktail was purchased from Roche (Laval, QC, Canada). RITC, Mouse isotype IgG1 (Clone MOPC-21), LPS (from *Salmonella typhosa*), PGE_2, phorbol myristate acetate (PMA), chloroquine, bafilomycin, Leu-Leu methyl ester hydrobromide (LLoME), Actinomycin D, Cyclohexamide and all other chemicals were purchased from Sigma-Aldrich (Oakville, ON, Canada).

2.2. Generation of the chitosan library

Chitosans (endotoxin units <500 $EU.g^{-1}$, protein content <0.2%, heavy metals < 5 ppm) with 82% DDA, block acetylation, and M_n 188 kDa (termed 80-190K-B), or 98% DDA and M_n 113 kDa (termed 98–110K) were provided by BioSyntech (now Smith & Nephew, Mississauga, ON, Canada). 98% DDA and 80% DDA block-acetylated chitosans with target M_n of 1, 3, 5 or 10 kDa were obtained through nitrous acid depolymerisation of the 98–110K and 80-190K-B chitosan, respectively, as previously described [19]. 60 and 80% DDA random-acetylated chitosans were generated from a starting chitosan (89.6% DDA and M_n 151 kDa) that was deacetylated to 98% DDA using two consecutive hot alkaline treatments (25% NaOH (w/v), 110 °C, 30 min), then nitrous acid-depolymerized to target M_n of 1, 3, 5 or 10 kDa. The 98% DDA chitosans with different M_n were reacetylated to 60 or 80% DDA using acetic anhydride as previously described [18]. The depolymerisation and reacetylation reactions were stopped by addition of 1 M NaOH until alkaline pH was reached. Alkaline-insoluble chitosans above 10 kDa precipitated and were extensively washed in double-deionized water (ddH_2O) by repeated centrifugation and resuspension until the supernatant reached neutral pH. Chitosans below 10 kDa were dialyzed (Biotech CE MWCO 100–500 Da, Spectrum Laboratories, CA, USA) five times against ddH_2O over 48 h. Free base chitosans were flash-frozen in liquid nitrogen and freeze-dried. Selected chitosans were labeled to 0.5% mol RITC per mol chitosan as previously described [20]. All reactions were performed using depyrogenized glassware and endotoxin-free reagents. Chitosans were characterized for DDA, M_n and weight-average molecular weight (M_w) using ^1H NMR and GPC as described previously [21,22]. PDI was calculated as M_w/M_n. Chitosans were solubilized at 5 mg mL^{-1} in dilute HCl (resulting in 90% protonation), 0.22 μm filter-sterilized and kept at −80 °C until use.

2.3. Macrophage differentiation and chitosan stimulation

All experiments involving human cell lines were carried out using institutionally approved protocols. U937 cells (ATCC # CRL-15932.2) were purchased from ATCC (Manassas, VA, USA), were maintained and differentiated to macrophages as described previously [6]. Briefly, U937 macrophages were differentiated in RPMI-1640 supplemented 10% FBS and 100 nM PMA for 72 h, manually resuspended, and seeded at 1×10^6 cells in 1 mL in 24-well plates in 100 nM PMA-containing medium overnight. Macrophages were stimulated for 24 h with 5, 50 or 150 μg/mL of each chitosan, or with 100 ng/mL LPS (positive control for inflammasome activation), 20 ng/mL IFN-γ (positive control for CXCL10 induction) or 20 ng/mL

IL-4 (positive control for IL-1ra induction without inducing IL-1β). In other experiments, macrophages were stimulated for 24 h in presence of 5 or 50 μg/mL 98-10K chitosan in presence of 100 μM chloroquine (reagent used to raise lysosomal pH), 100 nM bafilomycin (specific vacuolar H^+-ATPase pump inhibitor), PGE_2 (inflammasome mediator), or neutralizing antibodies against IFN-α or IFN-β. Following stimulation, the macrophage conditioned medium (CM) was centrifuged at 200 g for 10 min and stored at −80 °C until use.

2.4. Analysis of cell conditioned medium for cytokines, PGE_2 and Lactate dehydrogenase

Macrophage CM was analyzed by ELISA for IL-1β, IL-1ra, CXCL10 and PGE_2 concentration according to the manufacturer's instructions. Leakage of cytosolic Lactate dehydrogenase (LDH) into the macrophage CM was determined against an LDH standard curve using a colorimetric LDH assay (Clontech, Mountain View, CA, USA). Cytotoxicity was reported as the percentage of LDH leakage in the CM = (LDH activity in the CM of the sample)/(total LDH activity in the cell lysate and CM of control non-stimulated cells).

2.5. Immunoblotting

For analyses of STAT-1 and STAT-2 phosphorylation, cells were rinsed in cold PBS and lysed on ice in buffer containing 50 mM Tris, 150 mM NaCl, 2 mM Na_3VO_4, 10 mM NaF, 1% Triton-X 100 and protease inhibitors. For analysis of LC3 expression, cells were rinsed in cold PBS and lysed on ice in buffer containing 10 mM Tris, 150 mM NaCl, 0.04% Igepal CA-630, 2 mM EDTA, 0.5% sodium deoxycholate, 2 mM PMSF and protease inhibitors. Lysates were cleared by centrifugation at 21,000 g and kept at −80 °C until use.

40 μg of protein was separated by sodium dodecyl sulfate-polyacrylamide gel electrophoresis and transferred to PVDF membranes. Membranes were blocked for 1 h in 5% w/v BSA in Tris-buffered saline with Tween-20, probed overnight at 4 °C with primary antibody, and incubated with HRP-conjugated secondary antibodies for 1 h. Bands were detected using a chemiluminescent system (ECL, GE Healthcare, Baie d'Urfe, QC, Canada). β-Actin was used as a loading control. Band densitometry was carried out using Image J.

2.6. Immunohistofluorescence of Galectin-3, LC3 and confocal microscopy analyses

Macrophages were seeded in 8-chamber Labteks and stimulated with the 98-10K-RITC or 80-10K-R-RITC chitosans for 6, 10 or 18 h in presence or absence of 100 nM bafilomycin in medium with 100 nM PMA. Following stimulation, cells were fixed in ice-cold methanol for 15 min, incubated 1 h in 5% normal donkey serum/0.3% Triton-X 100/PBS, followed by overnight incubation at 4 °C with 5 μg/mL anti-Galectin-3 and 0.1 μg/mL Alexa Fluor 647-conjugated anti-LC3A/B, then further incubated with Alexa Fluor 488-conjugated donkey anti-mouse antibodies to detect mouse monoclonal anti-Galectin-3 for 1 h at room temperature. After washes in PBS, cells were counterstained with Hoechst 33342 and mounted in Mowiol.

Confocal imaging was performed using an Olympus FV1000 microscope using a 40× objective. Fluorophore signal detection was performed using sequential excitation/emission bandwith 405 nm/425–475 nm (Hoechst 33342), 488 nm/500–530 nm (Alexa Fluor 488), 543 nm/555–625 (RITC), 635 nm/650 nm (Alexa Fluor 647). Imaged cells were analyzed for the presence of Galectin-3/chitosan structures (GCS), which were identified as large intracellular punctated structures greater than 1.7 μm in diameter where RITC-chitosan and Galectin-3 were found to colocalize. For each condition, four random fields were analyzed per Labtek chamber and averaged to produce N = 4 measures per condition from 4 independent cultures.

2.7. Flow cytometry analysis

Macrophages were stimulated with 2.5 mM LLoME, 5 or 50 μg/mL 98-10K or 80-10K-R chitosan for 24 h. Cells were then stained with 100 nM LysoTracker for 2 h according to the manufacturer's instruction, washed, and analyzed using a FACSCalibur flow cytometer. Twenty thousand events were analyzed and data are reported as mean fluorescence intensity (MFI). The experiment was repeated in three independent cultures to generate N = 3 measures.

2.8. Statistical analyses

Data are shown as mean ± standard error of the mean. Statistical analyses were performed using Statistica (Statsoft, Tulsa, OK, USA). The Factorial ANOVA General Linear Model (GLM) with Fisher's Least Square Difference post-hoc analysis was used to determine differences in cytokine release, PGE_2 generation, and LDH leakage due to chitosan type and dose level as the categorical predictors (N = 4 independent cultures). The GLM with Fisher's Least Square Difference was used to determine differences in cytokine concentration, pSTAT-2/STAT-2 ratios, LC3-II/β-Actin band density, Lysotracker MFI, and GCS number as a function of treatment condition (98-10K chitosan, 80-10K-R chitosan, bafilomycin, chloroquine, neutralizing antibodies or PGE_2) (N = 3 to 4 independent cultures).

3. Results

3.1. Characterization of the chitosan library for structural features

Chitosan DDA was determined using the ratio of ^1H NMR peaks for H1D (5.2 ppm) and HAc (2.3 ppm) as previously assigned (Fig. 1) [22]. In comparison to the high molecular weight chitosans, proton spectra of the low molecular weight chitosans (below 5 kDa) showed additional peaks that were attributed to either protons on the 2,5-anhydro-D-mannose (M-unit) on the reducing end of the chitosan chain (3 peaks at 5.35, 4.5, 4.4 ppm) [23], or protons on a by-product of nitrous acid depolymerisation, hydroxymethyl furfural (HMF) (4 peaks at 9.7, 7.8, 6.9, 4.9 ppm) (Fig. 1) [24]. The library on average was within 1% (80%, 98%) or 5% (60%) of the target DDA. Gel permeation chromatography (GPC) analysis confirmed that the chitosan library was consistent with the target M_n, with a PDI ranging from 1.2 to 2.5 (Table 1). For simplicity, the chitosans used in this study were termed according to the nomenclature DDA-M_n-B (block-acetylated) or DDA-M_n-R (random-acetylated) (Table 1).

3.2. 98% DDA and 80% DDA block-acetylated chitosan stimulate differential IL-1ra/CXCL10 and PGE_2/IL-1β release in a dose-dependent manner

Using a 4-analyte factor array consisting in IL-1ra, CXCL10, IL-1β and PGE_2, two mutually exclusive cytokine response patterns were observed depending on the chitosan and dose. At lower dose levels (5, 50 μg/mL), 10–110 kDa 80% DDA block and 3–10 kDa 98% DDA chitosans induced CXCL10 and IL-1ra release (Fig. 2A and B). Paradoxically, chitosan induction of CXCL10 and IL-1ra tapered off as the dose was increased. At the highest chitosan dose (150 μg/mL), all 98% DDA chitosans over 3 kDa induced inflammasome activation, which led to increased IL-1β and PGE_2 release (Fig. 2C and D). IL-1β and PGE_2 release intensified as the molecular weight and dose of the >3 kDa 98% DDA chitosans increased (Fig. 2C and

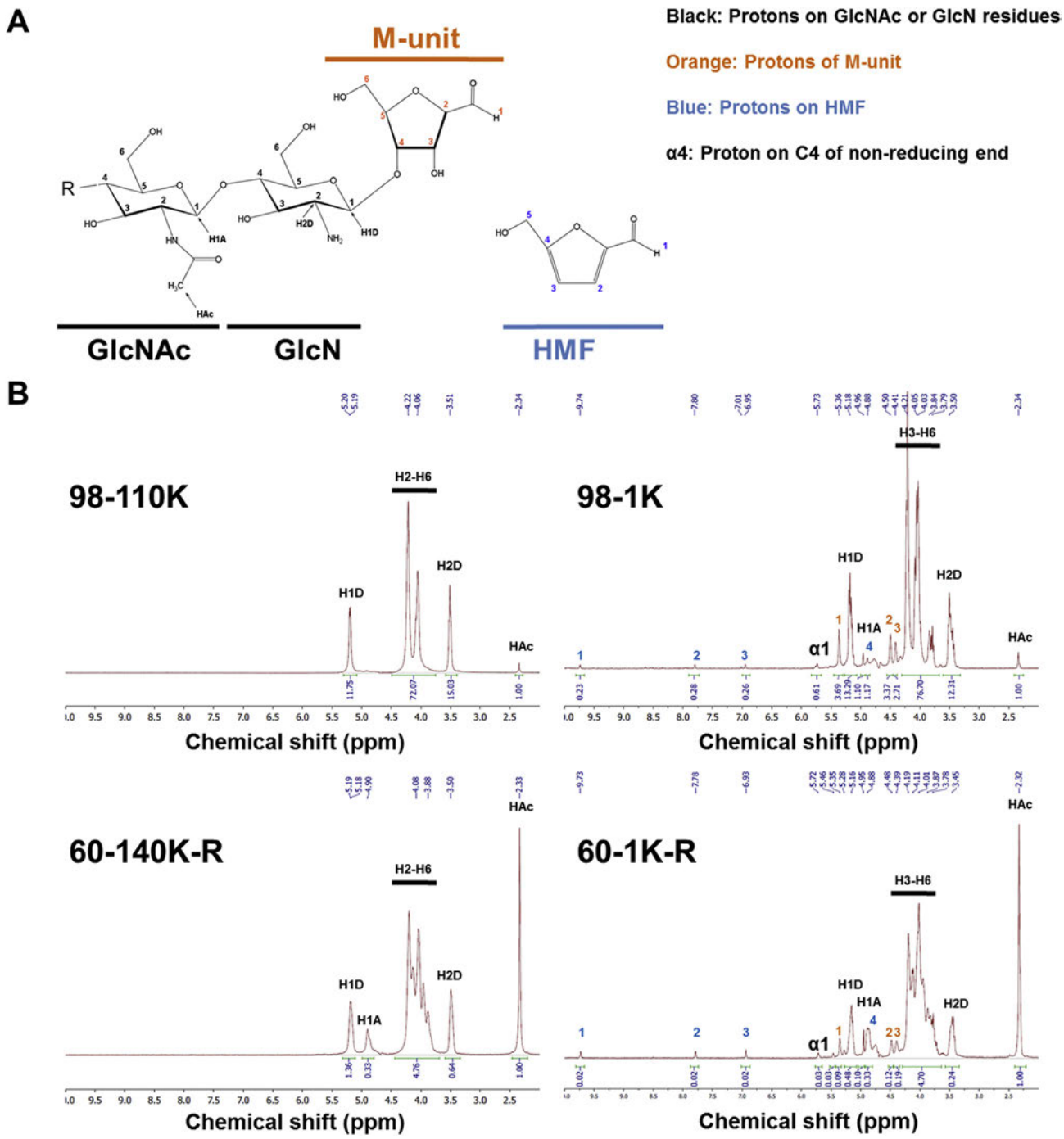

Fig. 1. Determination of chitosan DDA by ^{1}H NMR. A) Chemical representation of the reducing end of a chitosan chain showing the *N*-acetyl glucosamine (GlcNAc), glucosamine (GlcN) and anhydro-mannose (M-unit) subunits. The structure of hydroxymethylfurfural (HMF) is shown as well. The protons present on the GlcN and GlcNAc subunits are labeled in black, and the protons present on the M-unit and HMF are labeled in orange and blue, respectively. B) ^{1} H NMR spectrum of the 98−110K, 98-1K, 60-140K-R and 60-1K-R chitosans. Peaks labeled in black on the spectra are attributed to protons on the GlcNAc and GlcN subunits shown in A). Peaks labeled in orange or blue on the spectra are attributed to protons shown in A) on the M-unit or HMF molecule, respectively. The peak α4 is attributed to the proton of carbon 4 on the non-reducing end of the chitosan chain.

D). Random-acetylated chitosans and 1 kDa oligomers failed to induce any significant release of cytokines or PGE_2 (Fig. 2). In control cultures, IL-4 stimulated macrophages produced very high levels of IL-1ra compared to chitosan, and suppressed low-level baseline release of IL-1β (Fig. S1A). IFN-γ induced high levels of CXCL10, at 20-fold higher levels than the optimal dose of 98-10K chitosan (Fig. S1B), and slightly higher IL-1β over baseline. LPS was the only factor that induced IL-1β and PGE_2, and in addition induced the release of CXCL10 and even higher levels of IL-1ra than IL-4 (Figs. S1C and S1D). These data showed that chitosan-induced cytokine responses were distinct from those induced by IFN-γ, IL-4 or endotoxin. Therefore, more experiments were needed, to understand how selected chitosans at different doses could induce U937 macrophages to release either CXCL10 and IL-1ra, or IL-1β and PGE_2.

Cell cytotoxicity of the different chitosans and doses was

Table 1
Properties of the chitosans generated and tested in this study.

	Chitosan	DDA (%)	M_n (kDa)	PDI
98% DDA Chitosans	98-110K	98	113	2.0
	98-10K	99	9	1.2
	98-5K	99	4	1.6
	98-3K	99	3	1.5
	98-1K	98	1	1.3
80% DDA B-acetylated Chitosans	80-190K-B	82	188	2.2
	80-10K-B	83	11	1.5
	80-5K-B	81	5	1.8
	80-3K-B	83	3	1.1
	80-1K-B	80	1	1.5
80% DDA R-acetylated Chitosans	80-140K-R	80	144	1.8
	80-10K-R	80	11	1.4
	80-5K-R	81	5	1.5
	80-3K-R	81	3	1.5
	80-1K-R	81	1	1.3
60% DDA R-acetylated Chitosans	60-140K-R	65	152	1.7
	60-10K-R	62	16	1.3
	60-5K-R	53	4	1.6
	60-3K-R	59	3	2.5
	60-1K-R	61	1	1.8

determined by measuring LDH activity in the culture medium. LDH is a cytosolic enzyme released into the culture medium following cell death. LDH leakage induced by the library was found to parallel the level of IL-1β released to the medium, where the 98% DDA chitosans above 3 kDa at higher doses induced the most cell death (Fig. S2). Induction of IL-1β release, PGE_2 generation, and LDH leakage each correlated with chitosan tendency to precipitate and aggregate, as measured by chitosan turbidity at neutral pH ($R^2 = 0.69$ to 0.82, $p < 0.001$, Fig. S3).

In summary, our 4-analyte factor array showed that a sub-set of structurally distinct chitosans can induce the release of two distinct cytokine signatures: one signature consisted of co-induction of IL-1ra and CXCL10 at low chitosan doses ($R^2 = 0.72$, $p < 0.001$, Fig. S4A), and the other cytokine signature consisted of inflammasome activation (IL-1β and PGE_2 co-release; $R^2 = 0.93$, $p < 0.001$, Fig. S4B) at high chitosan concentrations.

3.3. Chitosan induces a type 1 IFN response to stimulate the release of IL-1ra and CXCL10

We previously reported that 132 kDa 82% DDA, block-acetylated chitosan induced delayed STAT-1 phosphorylation and CXCL10 secretion in U937 macrophages starting at 10 h post-stimulation [6]. In line with these observations, inhibition of translation or transcription prevented 80-190K-B chitosan from inducing STAT-1 phosphorylation (Fig. S5A), indicating that *de novo* gene expression was essential for the chitosan-induced STAT-1/CXCL10 response. Both type II (IFN-γ) and type I IFN (IFN-α/β) can induce STAT-1 factor activation leading to CXCL10 expression, however only IFN-α/β can induce STAT-2 phosphorylation [25]. We therefore used STAT-2 phosphorylation as a way to test whether chitosan was inducing type I IFN paracrine activity in our macrophage cultures. Conditioned medium (CM) collected from U937 cells stimulated for 1 h with 98-10K chitosan failed to induce STAT-1 or STAT-2 activation whereas 24 h-CM was able to specifically induce STAT-1 and STAT-2 phosphorylation in U937 cells, to a similar extent as CM from cells stimulated with IFN-α/β (Fig. 3A and B). Neutralization of IFN-β, but not IFN-α with blocking antibodies suppressed the ability of the 98-10K chitosan to induce STAT-2 phosphorylation (Fig. 3C–E) and to stimulate IL-1ra and CXCL10 release (Fig. 3F and G). Neutralization of IFN-β had no effect on IL-1β release (Fig. 3H). These data demonstrated that IFN-β is a paracrine factor induced by low doses of 98-10K chitosan that induces *de novo* STAT-1/STAT-2 activation and enhances CXCL10 and IL-1ra secretion.

It was previously reported that PGE_2 can inhibit IFN-α/β secretion, suggesting that the inflammasome serves as a feedback loop to shut down the type I IFN response in infected cells [26]. However, to our knowledge, it has never been reported that a biomaterial can induce this same feedback loop. U937 cells challenged with both 98-10K chitosan and increasing doses of PGE_2 showed that high doses of PGE_2 attenuated the ability of 98-10K chitosan to induce STAT-2 phosphorylation (Fig. 3D and E), CXCL10 production (Fig. 3F) and IL-1ra production (Fig. 3G). PGE_2 showed biphasic effects on IL-1β release in chitosan-stimulated cells, where the lowest dose of PGE_2 (0.1 μg/mL) potentiated IL-1β release, and the highest dose of PGE_2 (10 μg/mL) suppressed the effects of chitosan on this cytokine (Fig. 3H). Altogether, our data showed that chitosan elicited a type 1 IFN response by inducing IFN-β release, which was necessary and sufficient to induce CXCL10 and enhance IL-1ra production. Induction of the type 1 IFN response was suppressed by PGE_2 and mutually exclusive of chitosan-induced inflammasome activation.

3.4. Lysosomal rupture is critical for chitosan-elicited type 1 IFN response and inflammasome activation

Recent work reported a linear relationship between IFN-α/β production and early phagosomal rupture induced by *Mycobacterium tuberculosis* [27]. Others have also suggested lysosomal escape to be necessary for activation of the inflammasome by chitosan [5]. Some forms of endocytosed chitosan were shown to escape the lysosome through a proton-sponge effect. Due to chitosan's relatively high p*K*a value, 6.5, chitosan primary amines become protonated in the acidifying lysosomal lumen, leading to the accumulation of chloride ions and water. Subsequent lysosomal swelling results in the release of chitosan in the cytoplasm [28]. We therefore examined whether the chitosan-induced type 1 IFN response was dependent on lysosomal acidification. Following stimulation with Rhodamine Isothiocyanate-conjugated 98-10K chitosan (98-10K-RITC), we found that inhibiting lysosomal acidification using chloroquine or bafilomycin prevented the cytosolic diffusion of RITC-chitosan, and instead, the RITC-chitosan was confined to intracellular and extracellular vesicles (Fig. 4A). Furthermore, blockage of lysosomal acidification not only suppressed the effects of chitosan on inflammasome activation (IL-1β and PGE_2, Fig. 4B), it also suppressed the type 1 IFN cytokine response (IL-1ra and CXCL10, Fig. 4B). Suppression of the type I IFN response to chitosan was more sensitive to bafilomycin which blocks the proton pump than chloroquine which impedes acidification through a buffering action (Fig. 4B). These findings altogether confirmed that functional lysosomes were required not only for chitosan to activate the inflammasome and drive IL-1β release, but also to trigger the type 1 IFN response that promoted IL-1ra and CXCL10 release.

Our findings suggested that lysosomal rupture induced by chitosan is an essential initiating event of the type I IFN response. Lysosomal rupture is expected to trigger an autophagy response which can be measured by increased expression of LC3-II, the lipidated form of LC3 associated with newly formed autophagosomes [29]. We found that 98-10K chitosan induced LC3-II expression relative to β-actin in a dose-dependent manner (Fig. 4C and D). However, autophagy is a dynamic process and increased LC3-II could be explained by a net increase in autophagosome formation, or to an inhibition in autophagy flux. Blockage of autophagy flux with bafilomycin or chloroquine led to LC3-II accumulation that was not further enhanced by increasing doses of chitosan (Fig. 4C and D). These data refuted the hypothesis that chitosan induces a net increase in autophagosome formation.

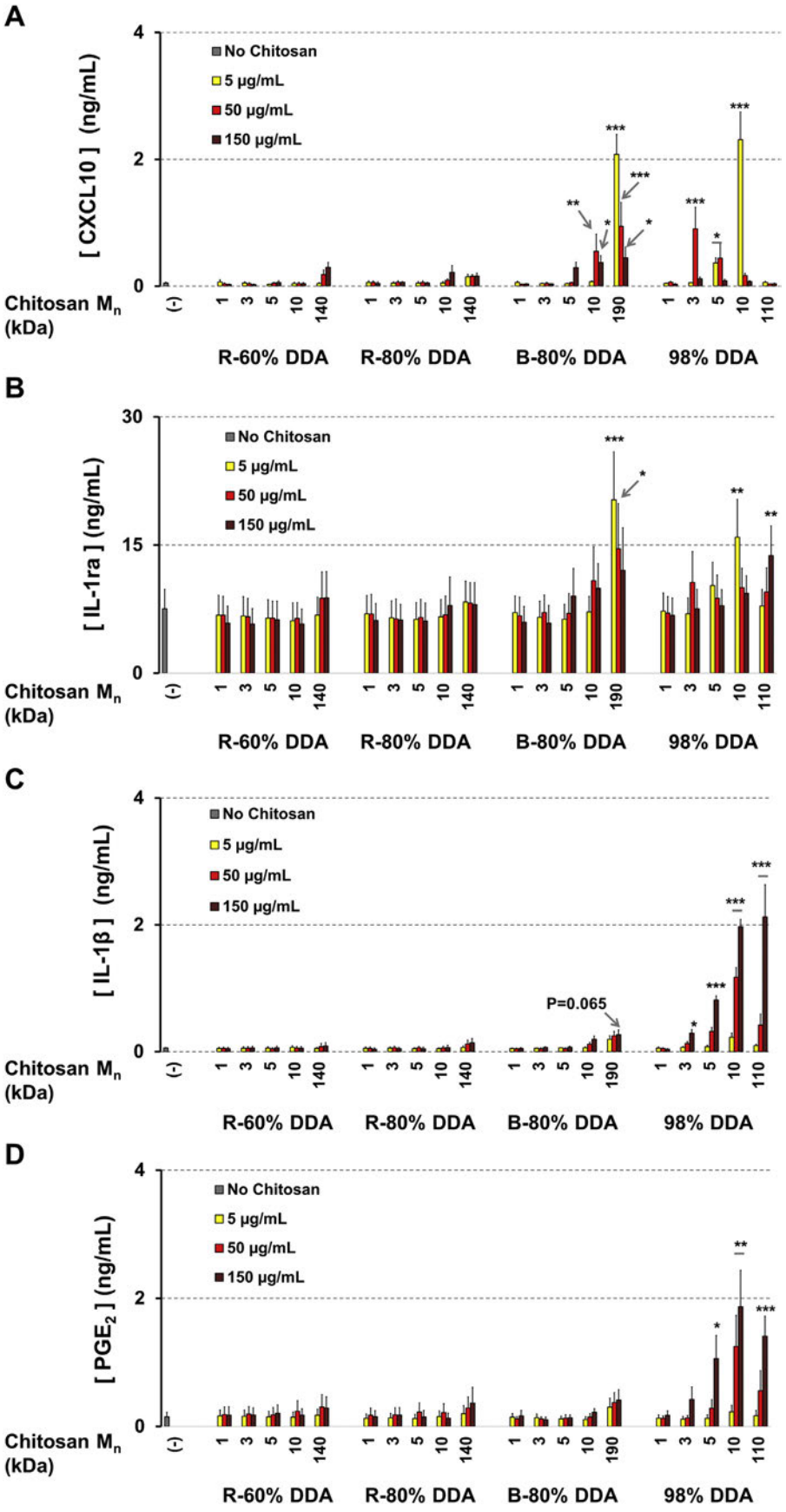

Fig. 2. Release of (A) CXCL10, (B) IL-1ra, (C) IL-1β and (D) PGE_2 from 1×10^6 macrophages stimulated for 24 h with the chitosan library. 98% DDA and 80% block-acetylated chitosans at low doses co-stimulated the release of (A) CXCL10 and (B) IL-1ra.98% DDA chitosans in a dose-dependent manner stimulated (C) IL-1β and (D) PGE_2 release. Random-acetylated chitosans and block-acetylated oligomers 80-5K-B, 80-3K-B and 80-1K-B failed to stimulate cytokine release. Data show mean ± standard error mean for n = 4 independent cultures. Significant differences between chitosan-treated cells and unstimulated cells (-): $^{*}p < 0.05$, $^{**}p < 0.01$, $^{***}p < 0.001$.

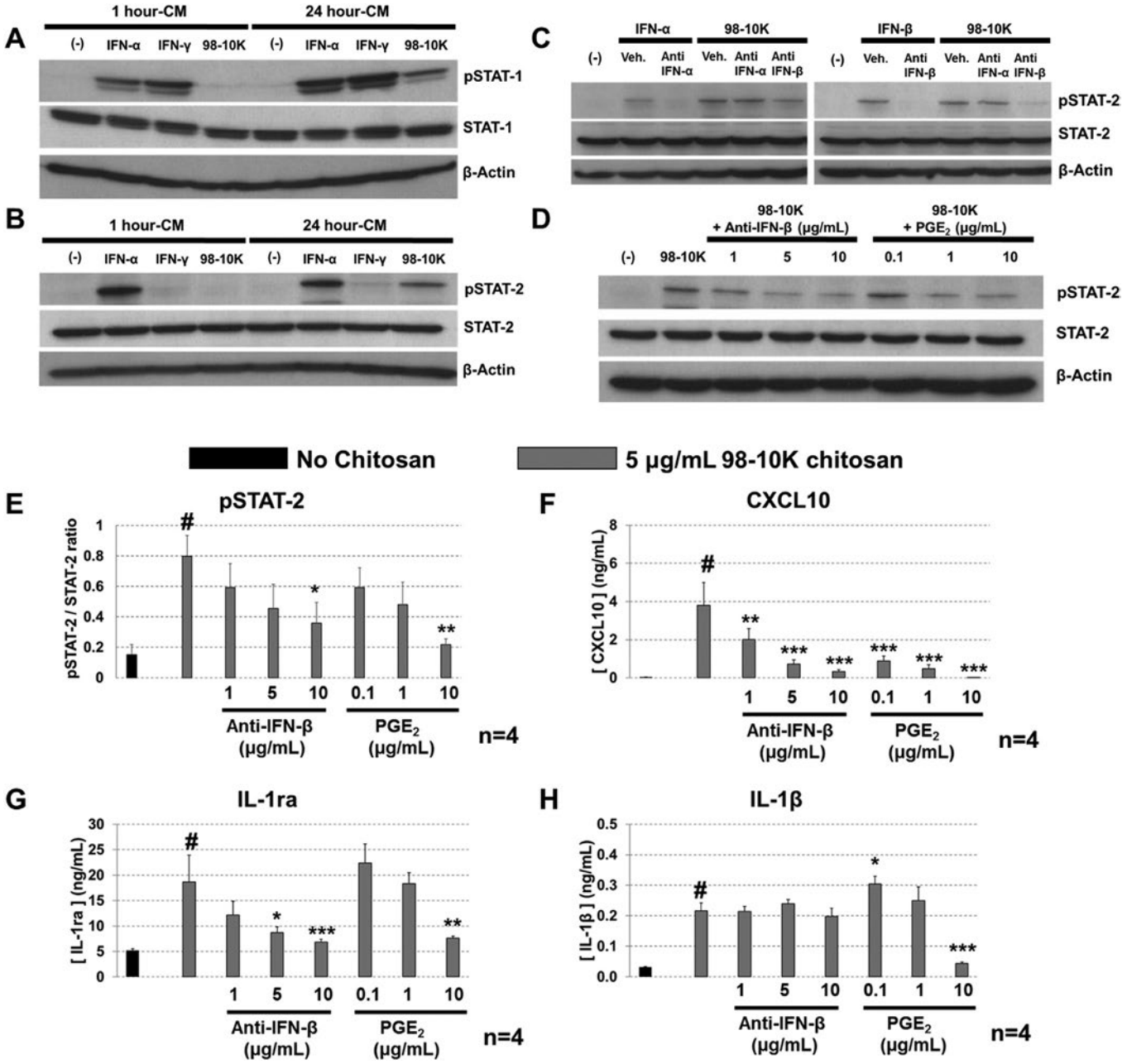

Fig. 3. Chitosan induces a delayed type 1 IFN cytokine response that involves paracrine IFN-β activity to stimulate IL-1ra and CXCL10 release. A) STAT-1 and B) STAT-2 western blots from lysates of U937 macrophages incubated for 1 h with conditioned medium from other U937 macrophages previously stimulated for 1 h (1 h-CM) or 24 h (24 h-CM) with 10 ng/mL IFN-α, 20 ng/mL IFN-γ, 5 μg/mL 98-10K chitosan. C) pSTAT-2 western blots from macrophages stimulated for 24 h with IFN-α, IFN-β or 5 μg/mL 98-10K chitosan in presence of neutralizing antibodies against IFN-α (Anti-IFN-α, 1 μg/mL) or IFN-β (Anti-IFN-β, 1 μg/mL). D) pSTAT-2 western blots and E) densitometric analyses of the ratio between phosphorylated and non-phosphorylated STAT-2 of macrophages stimulated for 24 h with 5 μg/mL of 98-10K chitosan in presence of increasing doses of Anti-IFN-β or PGE_2. F) IL-1ra, G) CXCL10 and H) IL-1β release from 1×10^6 macrophages stimulated for 24 h with 5 μg/mL of 98-10K chitosan in presence of increasing doses of Anti-IFN-β or PGE_2. Panels D–F: Data show mean ± standard error mean. #: $p < 0.01$ between non-stimulated cells and chitosan-stimulated cells alone; *$p < 0.05$, ***$p < 0.001$ between IFN-β or PGE_2 and 98-10K versus 98-10K alone.

Instead, these data suggested that chitosan created defective lysosomes that were incapable of fusing with autophagosomes, which led to slowed autophagy flux and higher LC3-II levels in chitosan-treated cells.

We next tested the hypothesis that lysosomal disruption is specific to chitosans that induce a type I IFN response. Intact lysosome levels in U937 cells, as measured by fluorescence intensity of cells loaded with LysoTracker, an acidotropic dye, were significantly decreased in macrophages stimulated with the 98-10K chitosan, and with the positive control LLoME (which induces lysosomal membrane rupture), but not with the 80-10K-R chitosan, a chitosan that failed to stimulate any cytokine responses (Fig. 5A and B).

To provide further evidence that chitosan 98-10K, but not 80-10K-R, induces lysosomal rupture, we looked at the distribution of galectin-3 in chitosan-stimulated macrophages. Galectin-3 and galectin-8 have been identified as cytosolic lectins that can sense and target vesicles damaged by intracellular pathogens through the interaction with glycoproteins that are normally inside the

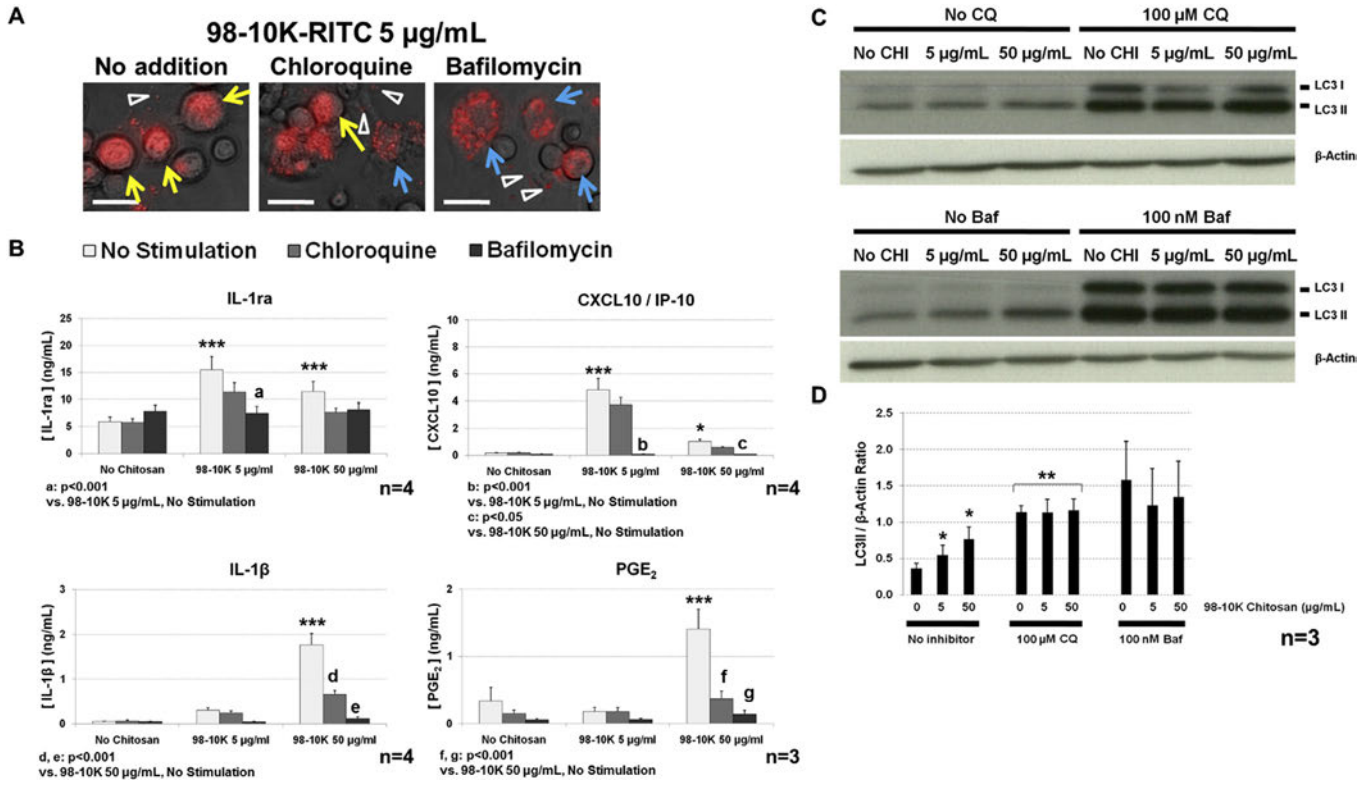

Fig. 4. Chitosan-induced cytokine responses are dependent on lysosomal acidification and are accompanied by slowed autophagy flux. A) Phase-contrast images of macrophages stimulated for 18 h with 5 μg/mL RITC-conjugated 98-10K chitosan in presence of 100 μM chloroquine or 100 nM bafilomycin. Yellow arrows show cells where RITC-chitosan is diffused in the cytosol. Blue arrows show cells where RITC-chitosan is in intracellular vesicles. White arrowheads show chitosan-containing extracellular vesicles. B) IL-1ra, CXCL10 and IL-1β release from 1×10^6 macrophages stimulated for 24 h with 5 or 50 μg/mL 98-10K chitosan alone, or in presence of chloroquine or bafilomycin. C) LC3 western blots from macrophages stimulated with 5 or 50 μg/mL 98-10K chitosan in presence of chloroquine or bafilomycin. D) Band densitometry showing LC3/β-Actin ratio of western blots shown in C). Scale bar = 10 μm. Data show mean ± standard error mean. Significant differences between chitosan-treated cells and unstimulated cells: $^{*}p < 0.05$, $^{***}p < 0.001$.

lysosome [30,31]. We hypothesized that galectin-3 colocalizes with the 98-10K-RITC chitosan, but not with the RITC-conjugated 80-10K-R (80-10K-R-RITC) chitosan, in a time-dependent manner. In unstimulated cells, galectin-3 was diffuse in the cytosol (Fig. 5C). We observed an accumulation of galectin-3 that colocalized with large punctated RITC-chitosan (Galectin-3/RITC-chitosan structures, "GCS") when macrophages were stimulated with the 98-10K-RITC chitosan, but not with the 80-10K-R-RITC chitosan (Fig. 5C and D), suggesting the lysosomes were specifically ruptured by the 98-10K chitosan. Significant levels of GCS were observed at 10 and 18 h post-stimulation with the 98-10K chitosan (Fig. 5D). Formation of these GCS was dependent on lysosomal acidification, confirming that 98-10K chitosan ruptured lysosomes through a proton sponge-dependent mechanism (Fig. 5D). Consistent with our previous observation suggesting that autophagosome accumulation was a result of chitosan-mediated lysosomal disruption (Fig. 4C and D), we found that cells stimulated with the 98-10K-RITC, but not 80-10K-R-RITC, showed accumulated LC3 punctates that either remained in the cytosol (Fig. 5E), or colocalized with GCS (Fig. S6). This altogether indicates that the differential capacity of the chitosans to elicit a type 1 IFN response or activate the inflammasome depends on the severity of lysosomal disruption once internalized.

4. Discussion

This study reports that a narrow range of chitosans (3–10 kDa, 98% DDA; 10 and 190 kDa, 80% DDA, block-acetylated) at low doses escape the lysosome and stimulate a delayed IFN-β paracrine response leading to STAT-1 and STAT-2 phosphorylation, *de novo* CXCL10 expression, and enhanced IL-1ra production. Our data suggest that the unique ability of selected chitosans at certain doses to induce this type 1 IFN response is related to their capacity to disrupt lysosomes as long as they do not induce significant inflammasome activation and cell death. Higher doses of chitosan, especially the 98% DDA chitosans that have greater neutral insolubility, were shown to induce inflammasome activation as marked by an IL-1β and PGE_2 response. McNab et al. recently proposed a model whereby macrophage infection by intracellular pathogens induces IL-1ra production through a IFN-α/β response that can compete and suppress the inflammasome mediator IL-1β, until excessive inflammasome activation produces PGE_2 release which suppresses IFN-α/β secretion [26]. Here, we demonstrate that like intracellular pathogens, at those concentrations that activate the inflammasome, chitosan particles induced high levels of PGE_2, which suppressed chitosan-mediated STAT-1/STAT-2 activation and CXCL10 release. Chitosan's ability to induce the type 1 IFN response was influenced by DDA, molecular weight and level of GlcNAc clustering. At 98% DDA, activation of the inflammasome was attenuated by decreasing molecular weight, which increases chitosan neutral-solubility and potentially limits the mass of chitosan internalized per phagosome. At 80% DDA, only the block-acetylated chitosans above 10 kDa stimulated a type 1 IFN response also suggesting that part of the requirements for chitosan to induce type I IFNs may depend on a minimal quantity of glucosamine chains (i.e., 3000 Da of consecutive glucosamine monomers) to be taken up by the phagosome.

In this work, we show that chitosan-mediated type 1 IFN response and inflammasome activation were mutually exclusive.

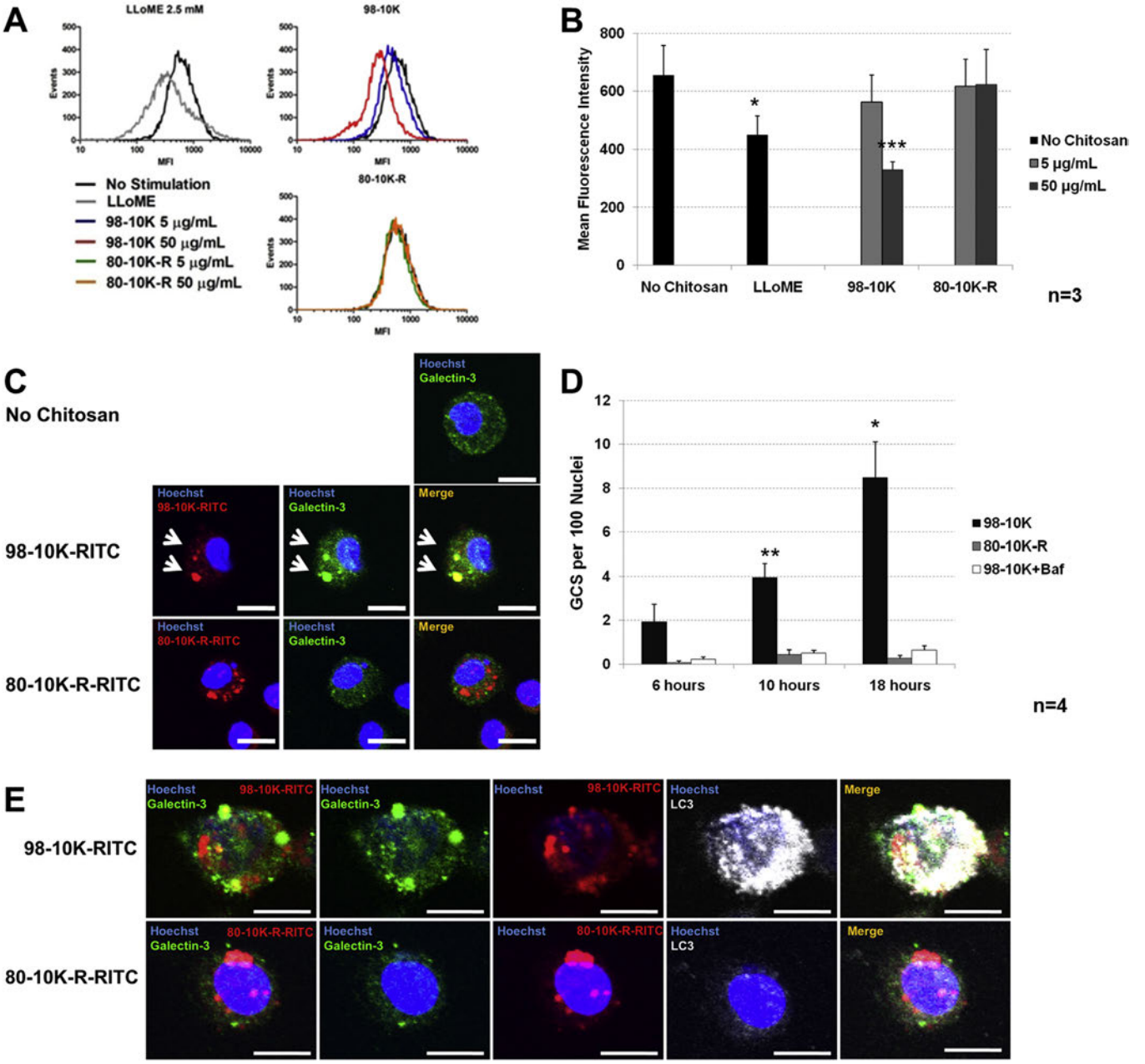

Fig. 5. Chitosans that stimulate cytokine release induce lysosomal disruption, which leads to galectin-3 recruitment to chitosan-containing vesicles and slowed autophagy flux. A) Flow cytometry histograms of macrophages stained with LysoTracker after 24 h of stimulation with 2.5 mM LLoME (a lysosomal disrupting agent), 5 or 50 μg/mL 98-10K or 80-10K-R chitosan. B) LysoTracker mean fluorescence intensity of macrophages stimulated with the different conditions shown in A). C) Confocal microscopy image showing Galectin-3 (green) and RITC-chitosan (red) localization in cells stimulated with the 98-10K-RITC (5 μg/mL) or 80-10K-R-RITC (50 μg/mL) chitosan after 18 h. White arrows indicate GCS. GCS were only detected when cells were stimulated with the 98-10K-RITC chitosan alone. D) Quantification of the number of GCS per 100 nuclei after 6, 10 and 18 h of stimulation. E) Confocal microscopy image showing Galectin-3 (green), RITC-chitosan, and LC3 (Grey) localization in cells stimulated with the 98-10K-RITC or 80-10K-R-RITC chitosan after 18 h. GCS and LC3 punctate formation were detected in cells stimulated with the 98-10K-RITC, but not the 80-10K-R-RITC chitosan. Data show mean ± standard error mean. Scale bar = 10 μm. Panel B) *p < 0.05, **p < 0.01, ***p < 0.001 *vs* non-stimulated cells. Panel D) *p < 0.05, **p < 0.01: 98-10K alone *vs* chitosan (80-10K-R or 98-10K) with bafilomycin.

Although these cytokine responses have been described in separate reports [4,5,32], our findings contribute significant insights on how these specific cytokine responses are linked, and more importantly how they are differentially elicited as a function of chitosan properties or dosage. For instance, the type 1 IFN response, which promotes IL-1ra and CXCL10 release, was restricted to specific chitosans applied at low doses. At higher doses, this response was abrogated and instead led to inflammasome activation. These novel findings suggest the possibility that chitosan dose and structural properties are tunable features that can be used to elicit or avoid specific macrophage immune responses to chitosan-based biomedical devices.

Our data showing critical effects of chitosan dose *in vitro* raise the important question on the potential effect of chitosan dose *in vivo*. Chitosans as micro- or nanoparticles were previously introduced *in vivo* in mice, rabbits, or sheep, at single or total dose that varied from 0.1 to 7 mg [32–38]. Interestingly, these chitosan doses *in vivo* were identified in our current study as inducing macrophage inflammasome activation *in vitro*. However, there are important differences between the *in vitro* and *in vivo* setting which

likely influence macrophage responses to chitosan. In our *in vitro* model, chitosan is delivered at a constant dose directly to macrophages for 24 h. This is different from the *in vivo* setting, where chitosan is delivered to tissues that contain variable levels of resident macrophages, recruited monocytes and other leukocytes, and chitosan concentration gradually decreases over time [39]. Little is known on the effect of chitosan dose on *in vivo* responses, mainly because we currently lack quantitative tools such as immunodetection or direct monitoring techniques to accurately measure chitosan concentration *in vivo*. However, our findings show that macrophage responses are highly sensitive to dose and suggest that chitosans delivered at doses capable of inducing macrophage inflammasome activation *in vitro* may become cleared or dispersed enough to lead to lower local chitosan concentrations, which may instead lead to a type 1 IFN response. This scenario is in fact supported by the observation that relatively high doses of chitosan adjuvant, 1 mg, elicit specific *in vivo* immune responses to H1 antigen (anti-H1 IgG2a production), but only in mice with a functional IFN-β receptor [32]. Our study highlights that in addition to chitosan structure, dose is another critical factor that can influence macrophage response to chitosan. Measuring the effects of chitosan dose and structure *in vivo* will be challenging and important to pursue in future studies.

Several studies have suggested that chitosan could be used to drive specific macrophage responses, such as M2 activation, that could be beneficial for wound repair [3,6,7,10,11]. However, identifying which chitosans lead to these responses has been a significant challenge due conflicting information in the literature. Indeed, chitosans with DDA between 80 and 95%, or varying molecular weights, have been reported in separate studies to either elicit either pro- [4–6,8,11,13,40,41], or anti-inflammatory macrophages responses [3,6,7,10,11]. These inconsistencies may stem from incomplete chitosan characterization [4,5,7,13,40], the different chitosan doses used across the different studies and the exclusive investigation of either only pro- or anti-inflammatory responses, which makes data interpretation difficult. Nonetheless, our data have revealed an interesting influence of chitosan solubility state on macrophage inflammatory responses. Based on our data, we predict that chitosans that are chemically modified to have higher neutral-solubility (i.e. PEGylated chitosan), and chitosans that induce strong PGE_2 will have little capacity to induce IFN-β, CXCL10 and higher IL-1ra release. Our study further predicts that chitosans that are more insoluble, highly deacetylated, and have a particle size amenable to phagocytosis will have a greater capacity to activate the inflammasome. Our findings bridge an important gap in the literature in identifying which chitosans will lead to inflammasome activation in macrophages, and which ones will not.

Chitosan likely activates immune cells through multiple mechanisms that are mostly unknown. Currently, there are two identified mechanisms involved in chitosan-mediated immune activation, the cGAS-STING/type 1 IFN pathway and NLRP3/inflammasome activation/IL-1β release [4,5,32]. We hypothesize that lysosomal rupture following chitosan phagocytosis is an essential initiating event that precedes both the cGAS-STING pathway and the inflammasome, and downstream cytokine responses. Firstly, our data show that the induction of CXCL10 secretion (i.e. 10 h, [6]) was paralleled by a time-dependent increase in lysosomal disruption (Figs. 4A, 5C and D). Lysosome rupture releases lysosomal contents, including proteases and glycosidases to the cytosol; after release to the cytosol some lysosomal proteases (cathepsins) are known to exert downstream effects on mitochondria [42]. Secondly, our data show that agents that block lysosomal acidification are sufficient to prevent chitosan-mediated cytokine responses, as bafilomycin prevented chitosan at different doses from inducing CXCL10 (Fig. 4B) or IL-1β release (Fig. 4B, [5]). Our data are consistent with the notion that mild levels of lysosomal disruption induced by chitosan lead to a type 1 IFN response, where paracrine IFN-β leads to intensified release of IL-1ra that can suppress low-level inflammasome induction of PGE_2 [26]. Conversely, chitosans that induced an overwhelming release of lysosomal content led to robust activation of the inflammasome and IL-1β secretion, which can out-compete extracellular IL-1ra leading to COX-2 activation, PGE_2 generation, and suppression of type 1 IFN secretion [26]. Mitochondrial-derived reactive oxygen species were suggested to be involved in the type 1 IFN response and inflammasome activation induced by a chitosan characterized as having 75–90% DDA and 150–400 kDa [5,32]; this chitosan preparation induced mitochondrial changes as early as 3 h after stimulation, which was followed by IFN-β release after 24 h [32]. Because in that previous study, the role of bafilomycin was not investigated, it would be interesting to test whether bafilomycin can prevent chitosan from inducing early mitochondrial changes in macrophages.

It is interesting to note that LC3-II co-localized with the GCS (Fig. S6). During bacterial intracellular infection, galectin-3, 8 and 9 detect damaged vesicles and galectin-8 targets them for autophagy as a means to restrict pathogen proliferation following infection [30,31]. Our results suggest that galectin-3 can sense vesicles damaged by chitosan and also provide evidence that chitosan-disrupted lysosomes are targeted to autophagosomes.

This study was conducted in a U937 macrophage model which was necessary for extensive screening of the chitosan library. The U937 cell model was chosen over primary macrophages partly because of the large numbers of cells required (>50 million cells per screen, and 4 distinct screening assays for $N = 4$), and partly because primary macrophages are known to exhibit donor-specific responses meaning primary cells would have required many replicates from potentially more than a single donor. It is important to note that U937 cells are transformed monocytic cells, and require PMA to terminally differentiate to macrophages. PMA enhances the expression of several genes involved in macrophage differentiation and function, including COX-2 and IRF-3/IRF-7 [43,44], which are critical for PGE_2 generation and type 1 IFN gene expression, respectively [43,44]. PMA also stimulates autophagy, phagocytosis and lysosomal activity [45,46], which are shown here and in previous studies to be important for chitosan-elicited cytokine responses [4,6]. Hence, PMA addition has an influence on macrophage responses to chitosan, especially since we previously showed that PMA-priming was necessary for chitosan (82% DDA, 132 kDa, block-acetylated) to induce CXCL10 expression in non-polarized human primary macrophages [6]. Our data now allow us to focus on specific chitosans for further analysis in primary cells and *in* vivo. Nevertheless, our findings are highly consistent, in terms of chitosan properties and concentration used, with previous studies showing that 80% DDA high molecular weight chitosans can activate the inflammasome in primary macrophages or elicit type 1 IFN responses in primary dendritic cells [4,5,32]. It is possible that chitosan may only trigger a type I IFN response *in vivo* when phagocytosed by activated macrophages. Primary dendritic cells produced *in vitro* by extended culture in GM-CSF were able to respond to a partly acetylated chitosan with IFN-β release [32]. In sum, these data suggest that to elicit type 1 IFN response *in vivo*, chitosan requires not only the right optimal structure and dose, but may also require tissue niches where GM-CSF or other cell polarization factors are present.

We found that low chitosan doses stimulate macrophages to release IL-1ra through paracrine type 1 IFN activity. In addition to using chitosan to induce type 1 IFNs for effective adjuvant effects in vaccines [32,37], our work suggests that chitosan-mediated type 1 IFN responses may have other important therapeutic benefits in the

context of regenerative medicine. Type 1 IFNs play important role in skin reepithelization following wounding [47]. Others have also shown that type 1 IFN promotes IL-1ra expression in liver tissues to yield a protective effect against fibrosis [48]. In osteochondral repair, IL-1ra is the physiological inhibitor of IL-1β, an important cytokine that contributes to the development of cartilage breakdown and osteoarthritis [49]. Although intra-articular type I IFN is detected in joints with chronic rheumatoid arthritis [50], IFN-β was previously tested in several clinical trials as a therapeutic to suppress joint inflammation [51]. Further work is needed to determine whether chitosan can be used to induce therapeutic type 1 IFN responses that are clinically beneficial for tissue engineering and wound repair.

5. Conclusion

The chitosan library generated in this study allowed us to identify the structural motifs required for chitosan to stimulate distinct cytokine responses in human macrophages. The minimal motif identified was 3 kDa of fully deacetylated chitosan, which is likely to be represented in the block 80% DDA 10 kDa and 190 kDa preparations. Specific chitosan preparations (10 or 190 kDa, block-acetylated 80% DDA; 3, 5 or 19 kDa, 98% DDA) stimulated two mutually exclusive cytokine responses as a function of chitosan dose which produced different levels of lysosomal disruption. Low chitosan doses induced mild lysosomal disruption to elicit a type 1 IFN response, which involved paracrine IFN-β activity and STAT-1/STAT-2 phosphorylation that led to IL-1ra and CXCL10 release. High levels of lysosomal disruption induced by higher chitosan doses activated the inflammasome which led to increased IL-1β, and PGE_2 release that suppressed the type 1 IFN response. These findings provide new advances in our understanding of the immunological properties of chitosan in macrophages, which will contribute to a better use of chitosan in widespread biomedical applications.

Author contribution

Conceptualization: DF, CDH, SS, ML; Methodology: DF, CDH, ML, PGG; Validation: DF, PGG, APC, TM, CDH; Investigation: DF, PGG, APC, TM; Formal analysis: DF, CDH; Writing – Original Draft: DF, CDH; Writing – Review & Editing: DF, CDH, SS; Visualization: DF, CDH; Supervision: CDH; Project Administration: CDH; Funding acquisition: CDH. All authors read and approved the final version of the manuscript.

Conflicts of interest

CDH is a shareholder, on the Board of Directors and holds a research contract with Ortho RTi, and holds funds from the Canadian Institutes of Health Research, Fonds de la Recherche en Santé du Québec and Natural Sciences and Engineering Council of Canada. SS holds funds from the Canadian Institutes of Health Research and Canadian Glycomics Networks (Networks of Centre of Excellence of Canada). ML is a shareholder of Ortho RTi. All other authors have no competing interests to declare.

Acknowledgements

We would like to thank Dr. Vincent Darras, Dr. Nicolas Tran-Khanh for experimental advice regarding to chitosan characterization and confocal microscopy analysis, Gaoping Chen and Jessica Guzman-Morales for technical assistance, and Julie Tremblay for quality assurance. This work was funded by the Canadian Institutes of Health Research (MOP 303615-BME). Salary support was from the Fonds de recherche du Québec – Santé (FRQ-S, National Researcher/Chercheur National, Grant No. 22341, CDH), Fonds de recherche du Québec – Nature et technologies (FRQ-NT, Ph.D. fellowship, DF), and NSERC summer scholarships (PGG, TM).

Appendix A. Supplementary data

Supplementary data related to this article can be found at http://dx.doi.org/10.1016/j.biomaterials.2017.03.022.

References

[1] I. Wedmore, J.G. McManus, A.E. Pusateri, J.B. Holcomb, A special report on the chitosan-based hemostatic dressing: experience in current combat operations, J. Trauma 60 (2006) 655–658.
[2] W.D. Stanish, R. McCormack, F. Forriol, N. Mohtadi, S. Pelet, J. Desnoyers, et al., Novel scaffold-based BST-CarGel treatment results in superior cartilage repair compared with microfracture in a randomized controlled trial, J. Bone Joint Surg. Am. Vol. 95 (2013) 1640–1650.
[3] C.D. Hoemann, G. Chen, C. Marchand, N. Tran-Khanh, M. Thibault, A. Chevrier, et al., Scaffold-guided subchondral bone repair: implication of neutrophils and alternatively activated arginase-1+ macrophages, Am. J. Sports Med. 38 (2010) 1845–1856.
[4] C.L. Bueter, C.K. Lee, V.A. Rathinam, G.J. Healy, C.H. Taron, C.A. Specht, et al., Chitosan but not chitin activates the inflammasome by a mechanism dependent upon phagocytosis, J. Biol. Chem. 286 (2011) 35447–35455.
[5] C.L. Bueter, C.K. Lee, J.P. Wang, G.R. Ostroff, C.A. Specht, S.M. Levitz, Spectrum and mechanisms of inflammasome activation by chitosan, J. Immunol. 192 (2014) 5943–5951.
[6] D. Fong, M.B. Ariganello, J. Girard-Lauziere, C.D. Hoemann, Biodegradable chitosan microparticles induce delayed STAT-1 activation and lead to distinct cytokine responses in differentially polarized human macrophages in vitro, Acta Biomater. 12 (2015) 183–194.
[7] H. Ueno, F. Nakamura, M. Murakami, M. Okumura, T. Kadosawa, T. Fujinag, Evaluation effects of chitosan for the extracellular matrix production by fibroblasts and the growth factors production by macrophages, Biomaterials 22 (2001) 2125–2130.
[8] J. Guzman-Morales, M.B. Ariganello, I. Hammami, M. Thibault, M. Jolicoeur, C.D. Hoemann, Biodegradable chitosan particles induce chemokine release and negligible arginase-1 activity compared to IL-4 in murine bone marrow-derived macrophages, Biochem. Biophys. Res. Commun. 405 (2011) 538–544.
[9] C.R. Almeida, T. Serra, M.I. Oliveira, J.A. Planell, M.A. Barbosa, M. Navarro, Impact of 3-D printed PLA- and chitosan-based scaffolds on human monocyte/macrophage responses: unraveling the effect of 3-D structures on inflammation, Acta Biomater. 10 (2014) 613–622.
[10] M.I. Oliveira, S.G. Santos, M.J. Oliveira, A.L. Torres, M.A. Barbosa, Chitosan drives anti-inflammatory macrophage polarisation and pro-inflammatory dendritic cell stimulation, Eur. Cell Mater 24 (2012) 136–153.
[11] D.P. Vasconcelos, A.C. Fonseca, M. Costa, I.F. Amaral, M.A. Barbosa, A.P. Aguas, et al., Macrophage polarization following chitosan implantation, Biomaterials 34 (2013) 9952–9959.
[12] C. Porporatto, I.D. Bianco, C.M. Riera, S.G. Correa, Chitosan induces different L-arginine metabolic pathways in resting and inflammatory macrophages, Biochem. Biophys. Res. Commun. 304 (2003) 266–272.
[13] S. Gudmundsdottir, R. Lieder, O.E. Sigurjonsson, P.H. Petersen, Chitosan leads to downregulation of YKL-40 and inflammasome activation in human macrophages, J. Biomed. Mater. Res. Part A 103 (8) (2015) 2778–2785.
[14] C. Gorzelanny, B. Poppelmann, K. Pappelbaum, B.M. Moerschbacher, S.W. Schneider, Human macrophage activation triggered by chitotriosidase-mediated chitin and chitosan degradation, Biomaterials 31 (2010) 8556–8563.
[15] G. Lamarque, C. Viton, A. Domard, Comparative study of the first heterogeneous deacetylation of alpha- and beta-chitins in a multistep process, Biomacromolecules 5 (2004) 992–1001.
[16] K.M. Varum, M.W. Anthonsen, H. Grasdalen, O. Smidsrod, High-field Nmr-spectroscopy of partially N-Deacetylated chitins (chitosans) .1. Determination of the degree of N-Acetylation and the distribution of N-Acetyl groups in partially N-Deacetylated chitins (chitosans) by high-field NMR-spectroscopy, Carbohydr. Res. 211 (1991) 17–23.
[17] S. Aiba, Studies on chitosan: 4. Lysozymic hydrolysis of partially N-acetylated chitosans, Int. J. Biol. Macromol. 14 (1992) 225–228.
[18] M. Lavertu, V. Darras, M.D. Buschmann, Kinetics and efficiency of chitosan reacetylation, Carbohydr. Polym. 87 (2012) 1192–1198.
[19] M. Lavertu, S. Methot, N. Tran-Khanh, M.D. Buschmann, High efficiency gene transfer using chitosan/DNA nanoparticles with specific combinations of molecular weight and degree of deacetylation, Biomaterials 27 (2006) 4815–4824.
[20] O. Ma, M. Lavertu, J. Sun, S. Nguyen, M.D. Buschmann, F.M. Winnik, et al., Precise derivatization of structurally distinct chitosans with rhodamine B isothiocyanate, Carbohydr. Polym. 72 (2008) 616–624.
[21] S. Nguyen, F.M. Winnik, M.D. Buschmann, Improved reproducibility in the

determination of the molecular weight of chitosan by analytical size exclusion chromatography, Carbohydr. Polym. 75 (2009) 528–533.
[22] M. Lavertu, Z. Xia, A.N. Serreqi, M. Berrada, A. Rodrigues, D. Wang, et al., A validated 1H NMR method for the determination of the degree of deacetylation of chitosan, J. Pharm. Biomed. Anal. 32 (2003) 1149–1158.
[23] H. Sugiyama, K. Hisamichi, K. Sakai, T. Usui, J.I. Ishiyama, H. Kudo, et al., The conformational study of chitin and chitosan oligomers in solution, Bioorg Med. Chem. 9 (2001) 211–216.
[24] K. Tommeraas, K.M. Varum, B.E. Christensen, O. Smidsrod, Preparation and characterisation of oligosaccharides produced by nitrous acid depolymerisation of chitosans, Carbohydr. Res. 333 (2001) 137–144.
[25] L.C. Platanias, Mechanisms of type-I- and type-II-interferon-mediated signalling, Nat. Rev. Immunol. 5 (2005) 375–386.
[26] F. McNab, K. Mayer-Barber, A. Sher, A. Wack, A. O'Garra, Type I interferons in infectious disease, Nat. Rev. Immunol. 15 (2015) 87–103.
[27] R. Simeone, F. Sayes, O. Song, M.I. Groschel, P. Brodin, R. Brosch, et al., Cytosolic access of Mycobacterium tuberculosis: critical impact of phagosomal acidification control and demonstration of occurrence in vivo, PLoS Pathog. 11 (2015) e1004650.
[28] M. Thibault, M. Astolfi, N. Tran-Khanh, M. Lavertu, V. Darras, A. Merzouki, et al., Excess polycation mediates efficient chitosan-based gene transfer by promoting lysosomal release of the polyplexes, Biomaterials 32 (2011) 4639–4646.
[29] D.J. Klionsky, H. Abeliovich, P. Agostinis, D.K. Agrawal, G. Aliev, D.S. Askew, et al., Guidelines for the use and interpretation of assays for monitoring autophagy in higher eukaryotes, Autophagy 4 (2008) 151–175.
[30] I. Paz, M. Sachse, N. Dupont, J. Mounier, C. Cederfur, J. Enninga, et al., Galectin-3, a marker for vacuole lysis by invasive pathogens, Cell. Microbiol. 12 (2010) 530–544.
[31] T.L. Thurston, M.P. Wandel, N. von Muhlinen, A. Foeglein, F. Randow, Galectin 8 targets damaged vesicles for autophagy to defend cells against bacterial invasion, Nature 482 (2012) 414–418.
[32] E.C. Carroll, L. Jin, A. Mori, N. Munoz-Wolf, E. Oleszycka, H.B. Moran, et al., The vaccine adjuvant chitosan promotes cellular immunity via DNA sensor cGAS-STING-dependent induction of type I interferons, Immunity 44 (2016) 597–608.
[33] M. Koping-Hoggard, K.M. Varum, M. Issa, S. Danielsen, B.E. Christensen, B.T. Stokke, et al., Improved chitosan-mediated gene delivery based on easily dissociated chitosan polyplexes of highly defined chitosan oligomers, Gene Ther. 11 (2004) 1441–1452.
[34] G.N. Shi, C.N. Zhang, R. Xu, J.F. Niu, H.J. Song, X.Y. Zhang, et al., Enhanced antitumor immunity by targeting dendritic cells with tumor cell lysate-loaded chitosan nanoparticles vaccine, Biomaterials 113 (2017) 191–202.
[35] C.D. Hoemann, A. Chenite, J. Sun, M. Hurtig, A. Serreqi, Z. Lu, et al., Cytocompatible gel formation of chitosan-glycerol phosphate solutions supplemented with hydroxyl ethyl cellulose is due to the presence of glyoxal, J. Biomed. Mater Res. A 83 (2007) 521–529.
[36] A. Chevrier, C.D. Hoemann, J. Sun, M.D. Buschmann, Chitosan-glycerol phosphate/blood implants increase cell recruitment, transient vascularization and subchondral bone remodeling in drilled cartilage defects, Osteoarthr. Cartil. 15 (2007) 316–327.
[37] M. Jean, F. Smaoui, M. Lavertu, S. Methot, L. Bouhdoud, M.D. Buschmann, et al., Chitosan-plasmid nanoparticle formulations for IM and SC delivery of recombinant FGF-2 and PDGF-BB or generation of antibodies, Gene Ther. 16 (2009) 1097–1110.
[38] A.D. Bell, V. Lascau-Coman, J. Sun, G. Chen, M.W. Lowerison, M.B. Hurtig, et al., Bone-induced chondroinduction in sheep Jamshidi biopsy defects with and without treatment by subchondral chitosan-blood implant: 1-day, 3-week, and 3-month repair, Cartilage 4 (2013) 131–143.
[39] C.D. Hoemann, D. Fong, 3-Immunological Responses to Chitosan for Biomedical Applications. Chitosan Based Biomaterials vol. 1, Woodhead Publishing, 2017, pp. 45–79.
[40] T. Mori, M. Murakami, M. Okumura, T. Kadosawa, T. Uede, T. Fujinaga, Mechanism of macrophage activation by chitin derivatives, J. Vet. Med. Sci. 67 (2005) 51–56.
[41] M. Otterlei, K.M. Varum, L. Ryan, T. Espevik, Characterization of binding and Tnf-alpha-inducing ability of chitosans on monocytes - the involvement of CD14, Vaccine 12 (1994) 825–832.
[42] M.E. Guicciardi, J. Deussing, H. Miyoshi, S.F. Bronk, P.A. Svingen, C. Peters, et al., Cathepsin B contributes to TNF-alpha-mediated hepatocyte apoptosis by promoting mitochondrial release of cytochrome c, J. Clin. Invest. 106 (2000) 1127–1137.
[43] R. Lu, P.M. Pitha, Monocyte differentiation to macrophage requires interferon regulatory factor 7, J. Biol. Chem. 276 (2001) 45491–45496.
[44] A. Medeiros, C. Peres-Buzalaf, F. Fortino Verdan, C.H. Serezani, Prostaglandin E2 and the suppression of phagocyte innate immune responses in different organs, Mediat. Inflamm. 2012 (2012) 327568.
[45] M. Daigneault, J.A. Preston, H.M. Marriott, M.K. Whyte, D.H. Dockrell, The identification of markers of macrophage differentiation in PMA-stimulated THP-1 cells and monocyte-derived macrophages, PloS One 5 (2010) e8668.
[46] S.D. Wright, S.C. Silverstein, Tumor-promoting phorbol esters stimulate C3b and C3b' receptor-mediated phagocytosis in cultured human monocytes, J. Exp. Med. 156 (1982) 1149–1164.
[47] J. Gregorio, S. Meller, C. Conrad, A. Di Nardo, B. Homey, A. Lauerma, et al., Plasmacytoid dendritic cells sense skin injury and promote wound healing through type I interferons, J. Exp. Med. 207 (2010) 2921–2930.
[48] Y.S. Roh, S. Park, J.W. Kim, C.W. Lim, E. Seki, B. Kim, Toll-like receptor 7-mediated type I interferon signaling prevents cholestasis- and hepatotoxin-induced liver fibrosis, Hepatology 60 (2014) 237–249.
[49] I. Iqbal, R. Fleischmann, Treatment of osteoarthritis with anakinra, Curr. Rheumatol. Rep. 9 (2007) 31–35.
[50] P.P. Tak, IFN-beta in rheumatoid arthritis, Front. Biosci. A J. Virtual Libr. 9 (2004) 3242–3247.
[51] J. van Holten, K. Pavelka, J. Vencovsky, H. Stahl, B. Rozman, M. Genovese, et al., A multicentre, randomised, double blind, placebo controlled phase II study of subcutaneous interferon beta-1a in the treatment of patients with active rheumatoid arthritis, Ann. Rheum. Dis. 64 (2005) 64–69.